International Conference on Renewable Energies and Power Quality (ICREPQ'13)
Bilbao (Spain), 20th to 22th March, 2013
Renewable Energy and Power Quality Journal (RE&PQJ)
ISSN 2172-038 X, No.11, March 2013

Thermal, mechanical and hydrodynamic analysis to optimize the design of molten salt central receivers of solar tower power plants.

M. R. Rodríguez-Sanchez[1*], M. Venegas-Bernal[1], C. Marugán-Cruz[1] and D. Santana[1].

[1] Department of Thermal and Fluid Engineering
Carlos III University of Madrid
Campus of Leganés, 28911 Madrid (Spain)
*Phone number: +0034 916246034, e-mail: mrrsanch@ing.uc3m.es

Abstract. One of the main problems of the molten-salt solar power tower plants is the reliability and lifetime estimation of central-receivers. The receiver must withstand high working temperatures, molten salt corrosion and important solar-flux transient thermal processes that lead to thermal stresses and fatigue. A thermal, mechanical and hydrodynamic analysis of the receiver has been carried out assuming constant temperature at each cell used in the simulations, but assuming axial and circumferential variation temperature in the whole perimeter of the receiver. The optimal design of this kind of receivers has been found varying the number of panels and the external diameter of the tubes. It has been obtained that the maximum film temperature and thermal stress follows a different evolution than the pressure drop, therefore it is necessary to make a compromise between them. The optimal receiver design must reduce the wall and film temperatures and the thermal stresses, assure the correct operation and prolong the lifetime of the receivers. In addition, the chosen design must have the highest thermal efficiency, reducing the number of heliostat and therefore the initial capital investment cost of the solar plant will be lower.

Key words

Solar power tower, Molten-salt Central-receiver, Film temperature, Thermal stresses, Pressure drop.

1. Introduction

Limited fossil fuel resources and severe environmental problems require new sustainable electricity generation options. Solar thermal power generation with optical concentration technologies are an important alternative for providing the clean and renewable energy needed in the future. The solar power tower technology (SPT), using molten salt as a heat transfer fluid, is known as one of the most promising technologies for producing solar electricity. A large thermal storage capability lets generate electric power with continuity and stability reducing the rate mismatch between energy supply and energy demand.

The SPT consists of three main systems: the heliostat field, solar collector and power block island. Direct solar radiation is reflected and concentrated by a heliostat field (individual mirrors with solar tracking system) onto a receiver placed at the top of a tower. In this way, the direct radiation is concentrated in the effective area of the receiver reaching a high peak of radiation. This solar energy is converted into thermal energy in the working fluid. In these systems, much attention has to be paid to the receiver because it is around 15% of the total capital investment cost of the plant. In addition, the receivers have the most uncertain lifetime due to the fact that the outer surface of the tubes intercepts directly the solar radiation, while the fluid which cools them flows on the inner part of the wall, causing tubes overheating and high thermal stresses.

In the present paper, an analysis of the central receivers has been carried out in order to optimize their design and increase their thermal efficiency.

2. Central solar receiver configuration.

The molten salt central receiver is configured as an external cylinder with vertical panels arranged on the surface to provide two parallel salt flow paths. The inlet flow enters at the north side of the receiver and it exits at the south side. The receiver is comprised of individual panel sections that include an inlet header, inlet nozzles, tubes, outlet nozzles, outlet header, tube clips, and panel support structures (Figure 1.left). The panels are supported at the top to permit unrestricted downward thermal expansion. To reduce the heat losses in the back side of the tubes, there is a thermal insulation (mineral wool) jacketed by a high reflectivity material, as white Pyromark, that seals the backside of the tubes [1].

The solar salt used is an off- eutectic mixture of 60% wt $NaNO_3$ and 40% wt KNO_3. The main characteristics of the molten salt are: high volumetric heat capacity and low conductivity, which are very desirable for thermal storage, and a great corrosion potential that presents a challenge for the heat exchange in the receiver. The tubes are generally built with stainless steel and nickel alloy to supports both, high temperatures and corrosive effects. For this study Alloy 800 has been used. Tube walls are coated with a high solar radiation absorptivity material (Pyromark 2500), which is stable at high temperatures and whose deformation behaviour is similar to the behaviour of the walls.

Nomenclature:

E: Modulus of elasticity.
F: View factor.
K: Expansion and contraction resistance coefficient.
NTU_z: Number of transfer units.
L_t: Tube length.
N_l: Number of lines in the receiver or salt paths.
N_p: Number of panels in the receiver.
R_o *and* R_1: Elbow radio.
S: Flow area.
T_{n+1}: Refractory wall temperature.
T_0: Environmental temperature.
$T_{salt,in}$: Inner salt temperature.
U: Global heat transfer coefficient.
d_o: Tube external diameter.
f_r: Darcy friction factor.
k: Thermal conductivity.
m: Mass flow rate in each element.
q_j: Heat flux absorbed by each section of tube.
q_{n+1}: Conduction losses through the refractory wall.
q_0: Radiation flux losses.
q_t: Heat flux absorbed by the tubes.
r_o *and* r_i: External and internal radio of the tubes, respectively.
t: Tube's thickness.
ΔP: Pressure drop.
ΔT: Radial temperature gradient.
α_t: Coefficient of thermal expansion.
α: Solar absorptivity.
δ: Surface of each section.
ε: Infrared emissivity.
ε_t: Thermal efficiency of the receiver.
ρ: Density of the salt.
ς: Poisson coefficient.
σ: Stefan-Boltzmann constant.
$\sigma_{eff,max}$: Maximum thermal stress.

It is important to identify three relevant temperatures to design a receiver:

1) Bulk temperature (T_{salt}): is the mean heat transfer fluid (HTF) temperature. It must be high enough to avoid HTF freezing and low enough to prevent the thermal decomposition of the HTF.
2) Tube external wall temperature (T_j *or* T_{outer}): Thermal losses by convection and radiation are related to this temperature. When the tube outer temperature increases excessively, corrosion under ambient condition increases too, the adherence of coating to metallic surfaces decreases and the thermal stresses increase even beyond the tube fatigue limit.
3) Film temperature (T_{film}): is the salt temperature of a thin layer near to the tube inner wall. This temperature is the highest temperature of the HTF in the receiver and is responsible of HTF stability. Furthermore, it is the temperature at which HTF corrodes tube material. A low increase of this temperature above certain limit can produce a sharp rise of the tube corrosion rate and stress corrosion cracking (SCC).

3. Receiver thermal modeling.

A. Design considerations.

The same parameters or, as similar as possible, to those in the SPT Solar 3, have been used in this study. The characteristics of the receiver are 10.5 m of length (H), a diameter (D) of 8.5 m and a thermal power of 120 MW.

The parameters used in this study are: the atmospheric conditions (30 °C of temperature, 1 bar of pressure, a relative humidity of 60% and a null wind velocity), the total mass flow rate (290 kg/s), which enters into the receiver at 290 ºC and exits at 565 ºC, and the tube thickness (1.65 mm). The variables of the problem are the number of panels and the tube external diameter.

The restrictions to assure the correct operation mode of the receiver are:

1) *Maximum film temperature*: It cannot be higher than 650 ºC in order to avoid corrosion of Alloy 800 and salt decomposition.
2) *Maximum thermal stresses:* to avoid fails due to fatigue it must be lower than 40% of the ultimate tensile strength (*UTS*).
3) *Maximum pressure drop:* 20 bar.

The method employed to solve the problem assumes constant tube wall temperature in each cell used in the numerical discretization. However, it considers temperature circumferential variations in the perimeter of the receiver, being the following step for the simulations found in the literature [2, 3].

In order to simplify the simulation, only one tube per panel has been simulated, although the effects of the adjacent tubes have been taken into account.

A representative receiver design formed by 18 panels and tubes external diameter of 4.22 cm has been used to show the main results in the followings sections.

B. Radiation map.

A two-dimensional normal distribution radiation map has been used as a model to carry out this analysis. The average heat flux of the model is 0.8 MW/m^2 and the maximum heat flux is 1.2 MW/m^2. (Figure 1.right).

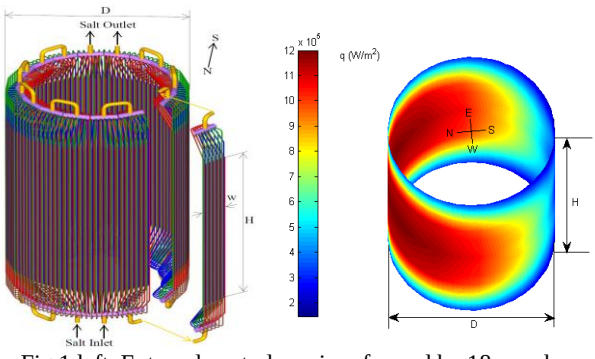

Fig.1.left. External central receiver formed by 18 panels.
Fig.1.right. Radiation map that arrives to the receiver.

C. Energy balance: heat flux.

Due to the high working temperatures of the salt and the high temperature of the tubes walls, not all the solar radiation that arrives from the heliostat is absorbed by the tubes, instead there are radiation, reflexion, convection and conduction heat losses.

Convective losses are caused by natural ($\overline{h_{nc}}$) and forced ($\overline{h_{fc}}$) convection, in this case forced convection is null due to there is not wind. The convective heat transfer coefficients have been calculated with the Siebers and Kraabel correlations as a function of the Nussel number (Nu) based on the diameter and on the length of the receiver [4]. The value of *Nu* is almost unchanged with the variation of the cosine angle over all circumferential direction for Reynolds (*Re*) and Prandtl (*Pr*) numbers around 17000 and 12, respectively [5].

$$\bar{h} = \left(\overline{h_{fc}}^{3.2} + \overline{h_{nc}}^{3.2}\right)^{\frac{1}{3.2}} = \overline{h_{nc}} \quad (1)$$

$$\overline{h_{nc}} = \frac{Nu_H \cdot k}{L_{tube}} \quad (2)$$

$$Nu_H = 0.098 Gr_H^{1/3} \left(\frac{T_w}{T_{amb}}\right) \quad (3)$$

Conductive losses in axial and circumferential direction can be neglected compared to the flux absorbed by the tubes. R*adiation and reflexion losses* are calculated at the same time than the heat flux absorbed by the tubes using the net radiation method (Equation 4), [6].

$$m = 0..n+1$$

$$\sum_{j=0}^{n}\left[\frac{\delta_{m,j}}{\varepsilon_j} - \left(\frac{1}{\varepsilon_j} - 1\right)F_{m-j}\right]\frac{q_j}{\sigma} - \left[\delta_{m,n+1} - F_{m-n+1}\right]T_{n+1}^{\ 4} = \quad (4)$$

$$= \sum_{j=0}^{n}\left[\delta_{m,j} - F_{m-j}\right]T_j^{\ 4} - \left[\frac{\delta_{m,n+1}}{\varepsilon_{n+1}} - \left(\frac{1}{\varepsilon_{n+1}} - 1\right)F_{m-n+1}\right]\frac{q_{n+1}}{\sigma} - F_{m-0}\frac{q_h}{\sigma}\alpha_i$$

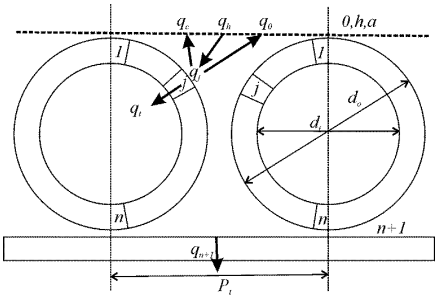

Fig. 2. Scheme with the most important parameters of the problem

In Equation 4, the refractory wall and the imaginary surface corresponding to the environment are represented by the subscripts n+1 and 0, respectively. Whereas the subscripts 1 to n denote the outer tube circular-sections as can be seen in the Figure 2. δ represents the area of each section, *F* corresponds to the view factor calculated by the crossed-strings method (a two-dimensional method that simplifies the simulations) [6]. The conduction losses through the refractory wall correspond to q_{n+1}. The radiation flux losses are represented by q_0 and the reflective losses are proportional to the last term of Equation 4. In addition, the heat flux absorbed by each tube is q_j (j=1...n), the solar heat flux from the heliostat field corresponds to q_h and the refractory wall temperature is T_{n+1}. The input parameters for Equation 4 are T_0 and T_j, being necessary to solve this using an iterative process.

Figure 3 shows, in one of the symmetric path of the salt for the representative receiver design of 18 panels and tubes external diameter of 4.22 cm, the evolution of the thermal power received from the heliostat (Q_h), the thermal power absorbed by the tubes (Q_t), as well as the heat losses due to reflection ($Q_{ref,l}$), radiation ($Q_{rad,l}$), convection ($Q_{c,l}$) and conduction ($Q_{k,l}$) as a function of the length of the tubes (L_t) multiplied by the number of panels of the receiver (N_p) and divided by the number of lines in the receiver (N_l). Horizontal axis starts on the north face of the receiver, where there is the maximum heat flux, and finishes on the south panel, where there is the minimum heat flux, as it was possible to see in Figure 1.right.

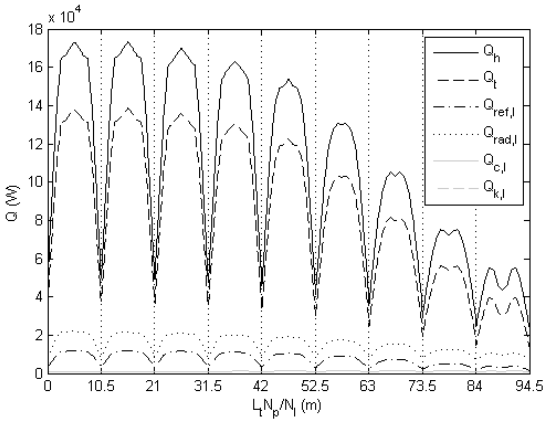

Fig. 3. Thermal power evolution in our representative receiver.

In Figure 3 it is possible to notice that the heat power along a tube is symmetric in the axial direction, being maximum at the centre of the tubes due to the shape of the radiation map. Furthermore, it can be seen that the radiation heat losses are the most important heat losses from the receivers, it is due to the consideration of circumferential temperature variations in the perimeter of the receiver.

D. Energy balance: temperatures.

Once the thermal power absorbed by the tubes has been obtained, it is possible to present an energy balance to obtain the bulk, the outer wall and the film temperature evolutions.

$$T_{salt}(z) = \bar{T}_j - \left(\bar{T}_j - T_{salt,in}\right)e^{-NTU_z} \quad (5)$$

$$T_j(z) = \frac{q_j}{U} + T_{salt}(z) \quad (6)$$

$$T_{film}(z) = T_j(z) - q_j \frac{r_o log\left(\frac{r_o}{r_i}\right)}{k} \quad (7)$$

Representing now these evolutions for our representative receiver design (Figure 4), from the north side to the south side of the receiver, it can be observed how the salt temperature increases from one panel to the other from 290 ºC to 565 ºC. However, the maximum film and the

outer wall temperatures (maximum, mean and minimum) have a symmetric form as thermal power. Moreover, their maximum value is obtained in the east/west panels of the receiver, being this part the critical point of the receivers.

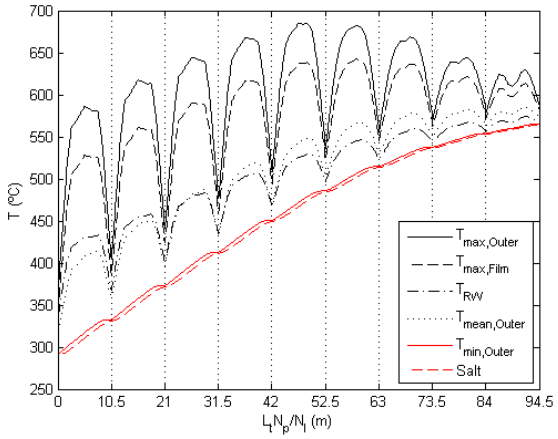

Fig. 4. Temperature evolution in our representative receiver.

At northern panels the heat flux is higher than on the rest, nevertheless, the salt is too cold to reach high temperatures. However, at the fifth panel, which corresponds to the west/east panels of the receiver, the heat flux continues being high and the salt temperature is high as well; therefore it is not capable of absorbing all the heat flux. As a result, the wall temperature increases. Finally, at the southern panels the heat flux is low, so in these panels the wall temperature is the lowest of the receiver.

In Figure 5 it is possible to see the axial and circumferential variations of film temperature. As the Figure 4 showed, the maximum film temperature is in the east/west side of the receiver, being higher in the external part of the receiver, whereas it is practically constant for the rest of circumferential angles.

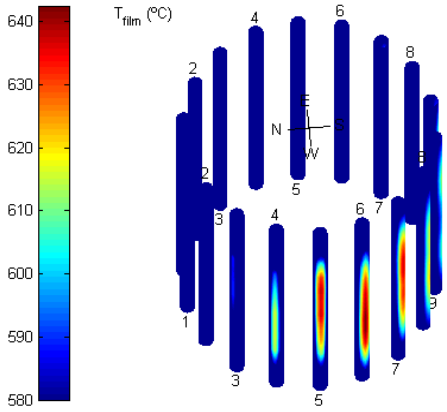

Fig. 5. Film temperature evolution in circumferential and axial directions for our representative receiver.

Finally, the most restrictive temperature of the problem, the maximum film temperature, has been studied as a function of the number of panels (from 16 to 26) and of the tube external diameter (from 1.37 cm to 6.03 cm) (Figure 6). The lowest temperature has been obtained for the highest number of panels and the smallest diameters.

Figure 6 shows that, with this receiver configuration, it is not advisable to use tubes of 6.03 cm of diameter, because the maximum film temperature reached is higher than 650 ºC. However, for diameters of 4.22 and 4.83 cm only receivers with high number of panels are valid and for the smallest diameters all the configurations are possible.

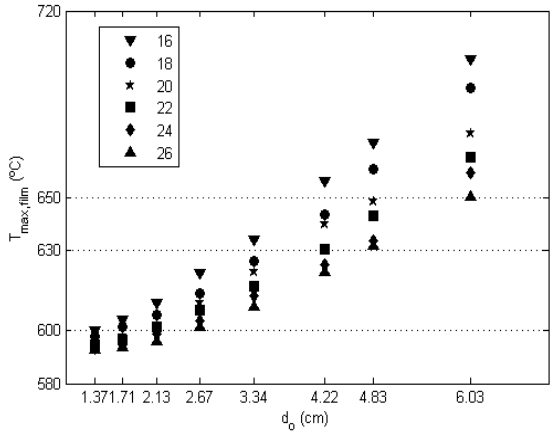

Fig. 6. Film temperature as a function of the number of panels and the diameter of the tubes of the receiver.

E. Thermal stresses.

The incident solar flux on the receiver produces temperature gradients through the tube wall large enough to develop plastic strains. Plastic strains are cumulative and the tubes will eventually fail due to low cycle fatigue. ASME Code Case N 47 [7] provided the Solar Two basis for calculating tube strains and fatigue life for a molten nitrate salt receiver operating at temperature ranges from 427 °C to 760 °C.

A tube of an external receiver has thermal stress in axial, radial and circumferential directions. The three directions of thermal stresses are independent between them [8]. In practice, axial and circumferential temperature gradients are almost one order of magnitude lower than the radial gradient, therefore only the radial stress has been considered in this study. Thereby, the governing thermal stress equations for radiant pipes [9] are:

$$\sigma_{eff,max} = \frac{\Delta T \alpha_t E}{2(1-\varsigma) ln\left(\frac{r_o}{r_i}\right)} \left(1 - \frac{2\, r_i^2}{r_o^2 - r_i^2}\right) ln\left(\frac{r_o}{r_i}\right) \sim \frac{E \alpha_t}{2(1-\varsigma) k} q_j t \qquad (8)$$

Where ΔT is the radial temperature gradient, r_o and r_i are the external and internal diameter of the tubes, respectively, and t is the tube thickness, that is 1.65 mm in all the cases studied.

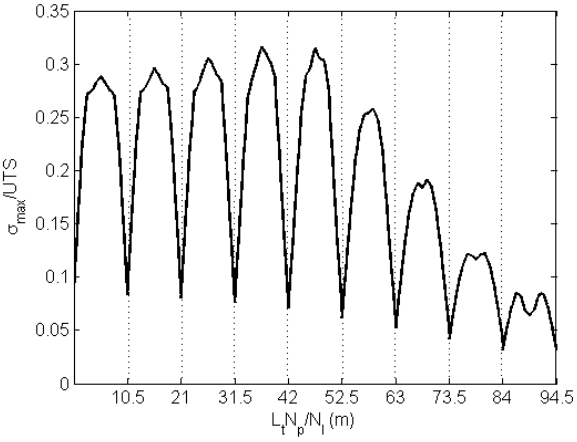

Fig. 7. Ratio maximum thermal stress - ultimate tensile strength evolution in our representative receiver.

In Figure 7 it is possible to see the evolution of the ratio thermal stress to ultimate tensile strength in our representative receiver. The trend of this parameter is similar to the wall and film temperature evolutions; on one hand it means that in a tube it is symmetrical respect to the axis direction, being maximum at the middle. And on the other hand the highest thermal stress occurs in the east/west side of the receiver. Therefore, it can be said that the mechanical and thermal critical points are the same.

Figure 8 represents the ratio maximum thermal stress to ultimate tensile strength as a function of the number of panels (from 16 to 26) and the tube external diameter (from 1.37 cm to 6.03 cm). It can be observed how thermal stress is independent on the number of panels, being a function of the heat flux absorbed by the tubes and therefore of the effective area of the receiver, which depends on the total number of tubes. Nevertheless, it is possible to observe that the highest tube diameter has the highest thermal stress, as occurred with film temperature.

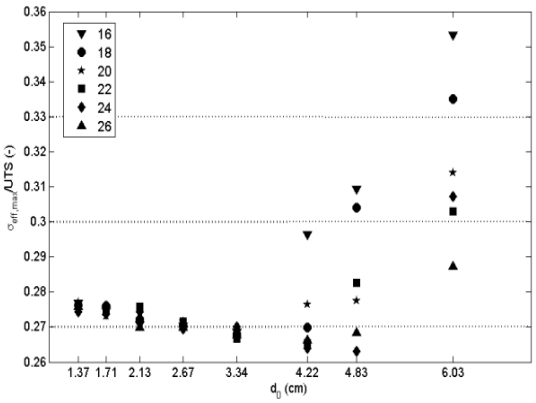

Fig. 8. Ratio maximum thermal stress - ultimate tensile strength as a function of the number of panels and the diameter of the tubes of the receiver.

Figure 8 shows that the thermal stresses are, for this flux radiation condition, lower than the limit imposed. Therefore, it can be concluded that, in this case, the optimal design will be chosen with the film temperature. The rest of variables will be studied in order to find other results and restrictions that help us to design the best receiver possible.

F. Pressure drop.

In this section the total pressure drop of the receiver has been calculated, including collectors, joints and the total number of tubes in the receiver, which are not completely straight (Figure 9). Therefore, it is possible to considerer that a receiver has straight zones, elbows, and abrupt expansions and contractions.

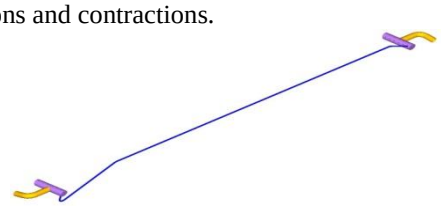

Fig. 9. Tube configuration in a receiver

Then, for smooth pipes with elbow curvature radius greater than the pipe internal diameter (R_0=0.13 m, R_1=0.2 m), the pressure drop in the receiver is obtained as the sum of the pressure drop of elbows, fitting and straight-pipe length as follows [10]:

$$\Delta P = \sum_{straight} f_r \frac{L}{d_o}\frac{\dot{m}^2}{2\rho S^2} + \sum_{exp/con} K \frac{\dot{m}^2}{2\rho S^2} + \sum_{elbow}\left[\left(1.3 - 0.29ln\frac{Re}{10^5}\right)0.21\left(\frac{R_o}{d_o}\right)^{-\frac{1}{4}} A_1\right]\frac{\dot{m}^2}{2\rho S^2} \quad (9)$$

Where A_1 is 0.45, 1 and 1.16 for 30º, 90º and 120º elbows, respectively. K is the expansion and contraction resistance coefficients [10] and f_r is the Darcy friction factor. f_r can be calculated explicitly for smooth and rough pipes using the correlations proposed by Romero et al. [11]. The fluid properties are calculated at the bulk temperature in each segment. S is the flow area.

Figure 10 shows the pressure drop as a function of the number of panels of the receiver (from 16 to 26) and the tube external diameter (from 1.37 cm to 6.03 cm).

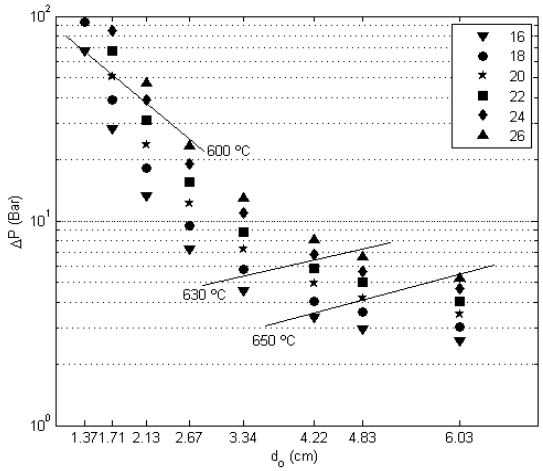

Fig. 10. Pressure drop as a function of the number of panels and the diameter of the tubes of the receiver.

It can be observed how the pressure drop increases with the number of panels, and decreases with the diameter of the tubes, opposite to the film temperature and thermal stresses. Therefore, a compromise between the different variables will be needed in order to design the best receiver configuration.

In addition, isothermal film temperature lines are represented in order to show the configurations no available for the limiting film temperature chosen. If film temperature limit decreases to 630 ºC or 600ºC other tube material as Inconel or stainless steel can be used in the receiver, but in these cases the configuration restrictions for the number of tubes and panels will be higher.

G. Thermal efficiency of the receiver.

Finally, the thermal efficiency of the receiver has been analysed. It is defined as the heat flux absorbed by the tubes (Q_t) divided between the heat flux from the heliostat (Q_h):

$$\varepsilon_t = \frac{\sum Q_t}{\sum Q_h} \quad (10)$$

The efficiency depends on the total number of tubes in the receiver (effective area). Figure 11 shows the

efficiency of the receivers as a function of the number of panels (from 16 to 26) and the tube diameter (from 1.37 cm to 6.03 cm). Additionally, it is possible to observe the film temperature, the total number of tubes and the material weight for several points.

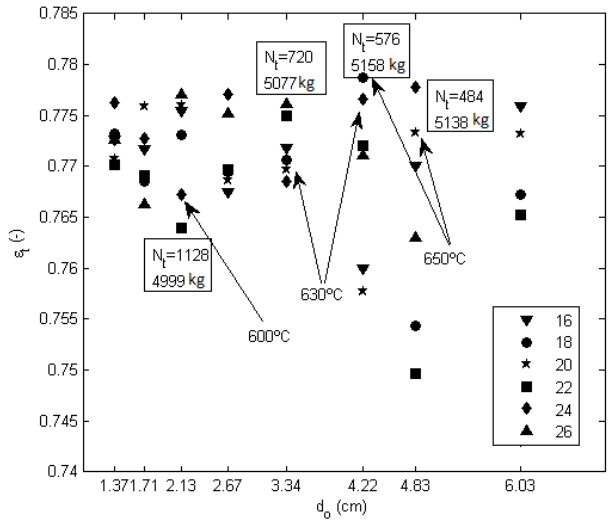

Fig. 11. Receiver's efficiency as a function of the number of panels and the diameter of the tubes of the receiver.

Figure 11 shows that the receiver efficiency is independent on the number of panels and on the tube diameter. However, it is a function of the total effective area. Figure 11 shows similar efficiencies for all the cases (near to 77%), except in the case of tube diameter equal to 4.83 cm where the efficiency is the lowest.

In order to design an optimal receiver, the ideal configuration will have the best efficiency as possible and a low number of tubes.

4. Conclusion

In this section, a summary of all the result obtained in this study will be done in order to obtain useful information.

First of all, the number of panels and the diameter of the tubes have a huge importance in the design of the receivers.

In all the cases studied the thermal and mechanical critical point of the receivers is at its east/west face, where the temperature of the walls increases, the film temperature exceeds its limit and the thermal stresses in the radial direction grow.

The optimal receiver design, from the viewpoint of the thermal and mechanical results, would use of a reduced number of panels and tubes of small diameters. However, small diameter tubes means great pressure drop and an extremely large number of tubes and clips and therefore, a bigger capital investment.

On the other hand, an elevated number of panels have high pressure drop and economical costs, because more headers and structural elements are needed.

Therefore, a compromise between the different variables will be needed in order to find an optimal receiver configuration. Taking into account thermal, mechanical and hydrodynamic result as well as the receiver thermal efficiency, the best receiver design, of 10.5 m of length and 8.5 m of diameter, is a receiver of 18 panels and 4.22 cm of tube external diameter. It means a total of 576 tubes and 5158 kg of Alloy 800 and a thermal efficiency near to 78%.

Acknowledgement

The author would like to thank the financial support for the project ENE2012-34255 and from CDTI and S2m Solutions for the project MOSARELA (Molten salt receiver lab) whose reference is IDI-20120128.

References

[1] Zavoico AB, "Solar power tower design basis document", Sandia National Laboratories, San Francisco, 2001.Rev.0., SAND 2001–2100.

[2] Csaba Singer, Reiner Buck, Robert Pitz-Paal, Hans Müller-Steinhagen, Assessment of Solar Power Tower Driven Ultrasupercritical Steam Cycles Applying Tubular Central Receivers With Varied Heat Transfer Media, Journal of Solar Energy Engineering, 2010, Vol. 132.

[3] Lu Jianfeng, Ding Jing, Yang Jianping, Heat transfer performance of an external receiver pipe under unilateral concentrated solar radiation, Solar Energy, 2010, Vol.84, pp. 1879-1887.

[4] Siebers DL, Kraabel JS, "Estimating Convective Energy Losses From Solar Central Receivers", Sandia National Laboratories, Albuquerque, 198, SAND 84-8717.

[5] Yang X, Yang X, Ding J, Shao Y, Fan H, "Numerical simulation study on the heat transfer characteristics of the tube receiver of the solar thermal power tower", Applied Energy 2012, Vol. 90, pp. 142-147.

[6] Modest M.F., Radiative Heat Transfer (2nd Edition), Elsevier, (2003).

[7] ASME Code Case N 47

[8] Fauple JH, Fisher FE. Engineering design–a synthesis of stress analysis and material engineering. New York, Wiley, 1981.

[9] Mohammad A. Irfan, Walter Chapman, "Thermal stresses in radiant tube due to axial, circumferential and radial temperature distributions". Applied Thermal Engineering 2009, Vol. 29, pp.1913-1920.

[10] Idelchik I.E, Handbook of Hydrodynamic Resistance, (3rd edition), Hemisphere Pub. Corp., (1986).

[11] Romeo E; Royo C; Monzon A, "Improved explicit equations for estimation of the friction factor in rough and smooth pipes", Chemical Engineering Journal 2002, Vol. 86, pp. 369-374.